Dyes and Pigments 86 (2010) 149–154

Contents lists available at ScienceDirect

Dyes and Pigments

journal homepage: www.elsevier.com/locate/dyepig

The influence of pyrrole linked to the π-conjugated polyene on crystal characteristics and polymorphism

Pil-Joo Kim [a], O-Pil Kwon [a,*], Mojca Jazbinsek [b], Hoseop Yun [c], Peter Günter [b]

[a] Department of Molecular Science and Technology, Ajou University, Suwon 443-749, Republic of Korea
[b] Nonlinear Optics Laboratory, ETH Zurich, CH-8093 Zurich, Switzerland
[c] Division of Energy Systems Research and Department of Chemistry, Ajou University, Suwon 443-749, Republic of Korea

ARTICLE INFO

Article history:
Received 17 October 2009
Received in revised form
17 December 2009
Accepted 21 December 2009
Available online 6 January 2010

Keywords:
Crystal engineering
Nonlinear optics
Isomerization
Polymorphism
Self-additive effect
Polyene

ABSTRACT

Novel pyrrole-based polyene derivatives bearing various different substituents were synthesized to investigate the influence of molecular conformational change (rotational isomerization) of a π-conjugated bridge on crystal characteristics and polymorphism. The pyrrole-based polyene crystals exhibited strong second harmonic generation efficiency that was ~two orders of magnitude larger than that of urea. Chromophores bearing asymmetric pyrrole readily formed polymorphs whereas crystals having a symmetric dimethylaminophenyl group displayed only one crystal structure. The observed polymorphism in pyrrole-based chromophores was attributed to the existence of rotational isomerization in which the minor rotamer exhibits a "self-additive effect" during the formation of the crystals.

1. Introduction

Organic crystal engineering is devoted to the design of a solid to achieve desired molecular orientation and physical properties, including crystal characteristics such as polymorphism, morphology and habit [1–5], for which, knowledge of the influence of molecular conformational change on crystal characteristics is important. Although the influences of molecular conformational changes in non-π-conjugated bridges on crystal characteristics have been extensively investigated [6,7], only a few studies discuss the influence conformational changes of π-conjugated bridges on crystal character, addressing mainly cis–trans isomerization [8,9], but rarely rotational isomerization.

Organic push–pull, π-conjugated, polyene molecules that posses both electron donor and electron acceptor groups have been extensively studied for photo- and electro-luminescent applications [10] and second-order nonlinear optical applications [11,12]. However, the low thermal and photochemical stability resulting from easy cis–trans isomerization of the polyene bridge presents serious limiting factors for many applications. To overcome this, configurationally locked polyene (CLP) chromophores having a plane-rigidified cyclohexene ring were developed [13–15]. Such CLP molecules can assume an acentric crystal structure, which is required for second-order nonlinear optics and exhibit large macroscopic second-order nonlinearity [16–18]. For example, the CLP chromophore having the dimethylaminophenyl electron donor, MM1 ((2-(3-(2-(4-dimethylaminophenyl)vinyl)-5,5-dimethylcyclohex-2-enylidene)malononitrile), see Fig. 1a) forms an acentric crystal structure with $P2_1$ space group and exhibits strong macroscopic nonlinearity [16].

To obtain acentric crystal structures for second-order nonlinear optical applications, understanding the conformational changes (i.e., isomerism) of the core molecular structure, namely the π-conjugated bridge of a typical nonlinear optical molecule, is a starting point for crystal engineering. A series of asymmetric, N-substituted pyrrole, nonlinear optical CLP chromophores having a pyrrole electron donor instead of a dimethylaminophenyl donor group were described [19], in which the existence of rotational isomerization [20] in the π-conjugated bridge was observed, typically in the single bond between the pyrrole and the hexatriene bridge, which links different types of π-conjugation (heteroaromatic ring and polyene) [19]. In quantum chemical calculations, the pyrrole-based CLP molecules show a strong asymmetry and a large angle $\theta(\mu,\beta)$ between the main charge-transfer direction

---

* Corresponding author. Tel.: +82 31 219 2462; fax: +82 31 219 1610.
E-mail address: opilkwon@ajou.ac.kr (O.-P. Kwon).

0143-7208/$ – see front matter © 2009 Elsevier Ltd. All rights reserved.
doi:10.1016/j.dyepig.2009.12.011

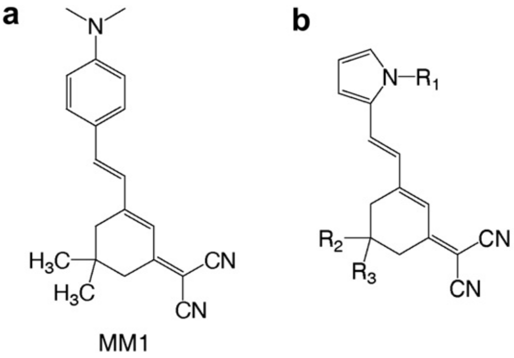

R_1	R_2	R_3	Abbr.
H	CH_3	CH_3	HP1
H	CH_3	H	HP2
H	H	H	HP3
CH_3	CH_3	CH_3	MP1
CH_3	CH_3	H	MP2
CH_3	H	H	MP3

Fig. 1. Chemical structure of the investigated pyrrole-based chromophore and their abbreviations.

β and the dipole moment μ. This is expected to reduce the probability for antiparallel arrangement of first hyperpolarizabilities in bulk materials [19] and therefore increase the probability for acentric crystal structures. To investigate acentric crystal-forming possibilities, new pyrrole-based CLP derivatives with different N-substituted groups (X: $-H$, $-CH_3$) on pyrrole and with different number of methyl substituents in cyclohexene ring have been designed and synthesized (see Fig. 1b). This paper concerns the influence of pyrrole linked to the π-conjugated polyene on crystal characteristics and polymorphism.

2. Experimental

2.1. Synthesis of chromophores

The pyrrole-based chromophores were synthesized using a condensation reaction with pyrrole-2-carbaldehyde or *N*-methyl-pyrrole-2-carbaldehyde and a corresponding intermediate, 2-(3,5,5-trimethylcyclohex-2-enylidene)malononitrile, 2-(3,5-dimethylcyclohex-2-enylidene)malononitrile, 2-(3-methylcyclohex-2-enylidene)malononitrile [16,19]. The synthesis of HP1 and MP1 were reported [19]; newly synthesized HP2, HP3, MP2, and MP3 were synthesized according to the literature [16,19]. For example, MP2: *N*-Methyl-pyrrole-2-carbaldehyde (3.11 mL, 29 mmol) was mixed with an equimolar amount of 2-(3,5-dimethylcyclohex-2-enylidene)malononitrile (5.0 g, 29 mmol) in ethanol (80 mL). With the catalyst piperidine, the solution was stirred for 16 h at room temperature. A crystalline solid obtained by filtration was purified by recrystallization in methylene chloride/methanol. In ^1H NMR spectra the chemical shifts (Varian 400 MHz NMR spectrometer) are reported in ppm (δ) relative to $(CH_3)_4Si$.

2-(5-Methyl-3-(2-(1-methyl-1H-pyrrol-2-yl)vinyl)cyclohex-2-enylidene)malononitrile (**MP2**) ^1H NMR ($CDCl_3$, δ): 1.20 (m, 3H, $-CH_3$), 2.04–2.10 (m, 1H, $-CH-CH_3$), 2.11–2.18 (m, 1H, $-CH_2$), 2.27–2.34 (m, 1H, $-CH_2$), 2.77–2.82 (m, 1H, $-CH_2$), 2.96–3.00 (m, 1H, $-CH_2$), 3.74 (s, 3H, $-NCH_3$), 6.23 (m, 1H, $-C{=}CH$), 6.69–6.78 (m, 3H, Py–H), 6.72–6.74 (d, 1H, $J = 16.0$ Hz, $-CH{=}CH$), 6.94–6.98 (d, 1H, $J = 16.0$ Hz, $-CH{=}CH-$). Elemental analysis for $C_{17}H_{17}N_3$: (%) Calcd. C 77.54, H 6.51, N 15.96; Found C 77.56, H 6.46, N 15.98. Yield: 44%.

2-(3-(2-(1-Methyl-1H-pyrrol-2-yl)vinyl)cyclohex-2-enylidene) malononitrile (**MP3**) ^1H NMR ($CDCl_3$, δ): 1.97 (m, 2H, $-CH_2$), 2.62 (t, 2H, $J = 12$, $-CH_2$), 2.79 (t, 2H, $J = 12.8$, CH_2), 3.73 (s, 3H, $-NCH_3$), 6.23 (m, 1H, $-C{=}CH$), 6.69–6.78 (m, 3H, Py–H), 6.71–6.75 (d, 1H, $J = 16.4$ Hz, $-CH{=}CH$), 6.94–6.98 (d, 1H, $J = 15.6$ Hz, $-CH{=}CH-$). Elemental analysis for $C_{16}H_{15}N_3$: (%) Calcd. C 77.08, H 6.06, N 16.85; Found C 77.04, H 6.09, N 16.75. Yield: 15%.

2-(3-(2-(1H-pyrrol-2-yl)vinyl)-5-methylcyclohex-2-enylidene) malononitrile (**HP2**) ^1H NMR ($CDCl_3$, δ): 1.16 (m, 3H, $-CH_3$), 2.0–2.15 (m, 2H, $-CH_2$), 2.28 (m, 1H, $-CH-CH_3$), 2.77 (d, 1H, $-CH_2$), 2.94 (d, 1H, $-CH_2$), 6.31 (m, 1H, $-C{=}CH-$), 6.51 (d, 1H, $J = 16.0$ Hz, $-CH{=}CH-$), 6.55 (m, 1H, Py–H), 6.68 (s, 1H, Py–H), 6.96 (d, 1H, $J = 15.6$ Hz, $-CH{=}CH-$), 6.99 (s, 1H, Py–H), 8.68 (s, 1H, NH). Elemental analysis for $C_{16}H_{15}N_3$: (%) Calcd. C 77.08, H 6.06, N 16.85; Found C 77.02, H 6.02, N 16.79. Yield: 12%.

2-(3-(2-(1H-pyrrol-2-yl)vinyl)cyclohex-2-enylidene)malononitrile (**HP3**) ^1H NMR ($CDCl_3$, δ): 2.0–2.15 (m, 2H, $-CH_2$), 2.28 (m, 1H, $-CH-CH_3$), 2.77 (d, 1H, $-CH_2$), 2.94 (d, 1H, $-CH_2$), 6.31 (m, 1H, $-C{=}CH-$), 6.51 (d, 1H, $J = 15.6$ Hz, $-CH{=}CH-$), 6.55 (m, 1H, Py–H), 6.68 (s, 1H, Py–H), 6.96 (d, 1H, $J = 16.0$ Hz, $-CH{=}CH-$), 6.99 (s, 1H, Py–H), 8.68 (s, 1H, NH). Elemental analysis for $C_{15}H_{13}N_3$: (%) Calcd. C 76.57, H 5.57, N 17.86; Found C 76.61, H 5.56, N 17.83. Yield: 21%.

2.2. Absorption and photoluminescence measurement

UV/vis. absorption and photoluminescent spectra in solution were recorded by a Jasco V-570 and FP-6500 spectrometer, respectively. Photoluminescence spectra in solid state were measured using a custom built luminescence spectrometer based on an OceanOptics USB4000 CCD spectrometer (range: 350–1000 nm) for detection and a green cw laser with 532 nm for excitation.

2.3. X-ray crystallographic data

2.3.1. HP2-III

$C_{17}H_{19}N_3O$, $M_r = 281.35$, triclinic, space group P_1, $a = 8.4670(5)$ Å, $b = 8.7508(6)$ Å, $c = 12.3055(7)$ Å, $\alpha = 106.224(2)^\circ$, $\beta = 91.827(2)^\circ$, $\gamma = 112.269(2)^\circ$, $V = 800.36(8)$ Å^3, $Z = 2$, $T = 290(2)$ K, $\mu(MoK\alpha) = 0.075$ mm^{-1}. Of 7871 reflections collected in the θ range 3.14°–27.45° using an ω scans on a Rigaku R-axis Rapid S diffractometer, 3635 were unique reflections ($R_{int} = 0.018$, completeness = 99.1%). The structure was solved and refined against F^2 using SHELX97 [21], 192 variables, $wR_2 = 0.1432$, $R_1 = 0.0468$ ($F_o^2 > 2\sigma(F_o^2)$), GOF = 1.123, and max/min residual electron density 0.716/−0.265 eÅ^{-3}, CCDC-733790.

2.3.2. MP3-II

$C_{16}H_{15}N_3$, $M_r = 249.32$, triclinic, space group P_1, $a = 6.9858(5)$ Å, $b = 7.4647(5)$ Å, $c = 13.4359(11)$ Å, $\alpha = 87.512(3)^\circ$, $\beta = 80.833(3)^\circ$, $\gamma = 81.2109(17)^\circ$, $V = 683.44(9)$ Å^3, $Z = 2$, $T = 293(2)$ K, $\mu(MoK\alpha) = 0.072$ mm^{-1}. Of 6390 reflections collected in the θ range 2.0°–27.5° using an ω scans on a Rigaku R-axis Rapid S diffractometer, 3026 were unique reflections ($R_{int} = 0.0171$, completeness = 96.9%). The structure was solved and refined against F^2 using SHELX97 [21], 173 variables, $wR_2 = 0.1721$, $R_1 = 0.0477$ (1778 reflections having $F_o^2 > 2\sigma(F_o^2)$), GOF = 1.080, and max/min residual electron density 0.329/−0.238 eÅ^{-3}. CCDC-733791.

3. Results and discussion

3.1. Rational design of pyrrole-based chromophores

Fig. 1 shows the chemical structures of the investigated pyrrole-based chromophores. The chromophores consist of the π-conjugated configurationally locked polyene bridge linked to pyrrole electron donor and dicyanomethylidene electron acceptor. Since dicyanomethylidene electron acceptor group can also act as hydrogen bond acceptor, we choose un-substituted pyrrole and *N*-methyl-pyrrole on the electron donor site to introduce different intermolecular hydrogen bonds in solid state. We also varied the number of methyl substituents on the cyclohexene ring because crystal structures can strongly depend on the number of the methyl substituents in CLP crystals [17].

The wavelength of maximum absorption λ_{max} of the synthesized chromophores with un-substituted pyrrole and *N*-methyl-pyrrole groups are similar; about 470 nm in the methanol solution. As expected, this suggests that the substituents introduced do not considerably affect the electronic molecular properties and molecular nonlinearity, and may only be important for crystal formation characteristics. All pyrrole-based chromophores exhibit high thermal stability; the initial weight-loss temperature T_i of about 270 °C at the heating rate of 10 °C/min was determined by thermogravimetric analysis (TGA) measurements.

To screen the macroscopic nonlinearity, the Kurtz and Perry powder second harmonic generation (SHG) test was performed at the fundamental wavelength of 1.9 μm with crystalline powders obtained from methylene chloride (MC)/methanol solution by slow evaporation method. Among the six pyrrole-based compounds, HP2 and MP3 crystals exhibited a strong SHG efficiency: 2.2 times and 1.3 times larger than that of MM1 powder, which is about two orders of magnitude larger than urea [16]. Therefore, HP2 and MP3 chromophores may pack in acentric structures promising for second-order nonlinear optical applications.

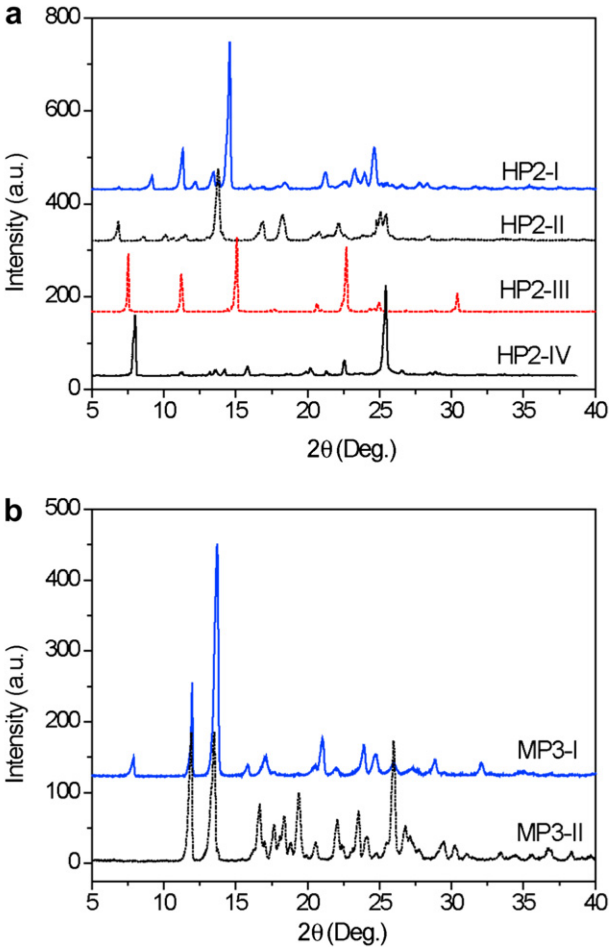

Fig. 2. Powder X-ray diffraction patterns for polymorph crystals of HP2 (a) and MP3 (b).

3.2. Crystal characteristics and polymorphism

Crystal-forming characteristics were investigated in more detail for HP2 and MP3 due to the observed large macroscopic nonlinearity. We grew crystals from different solvents and characterized their properties by differential scanning calorimetry (DSC), X-ray diffraction, powder SHG test and photoluminescence. The crystal growing method and the physical properties of several HP2 and MP3 polymorphs obtained are listed in Table 1. We obtained four polymorphs of HP2 and two of MP3, whose presence was confirmed by powder X-ray diffraction (see Fig. 2). HP2-III and HP2-IV crystals include a solvent, methanol and methyl ethyl ketone (MEK), respectively, as determined by ^{1}H NMR measurement. In the powder SHG test, HP2-I and MP3-I phases are SHG active, while the other HP2 and MP3 polymorphs are SHG inactive. Therefore, HP2-I

Table 1
Growth method, physical, and chemical data of CLP crystals: λ_{abs} is the wavelength of the maximum absorption in methanol solution, $\lambda_{em,solution}$ and $\lambda_{em,solid}$ are the wavelength of the maximum emission in methanol solution and solid, respectively, T_{tr} the phase transition temperature, and T_m the melting temperature (peak position in DSC scan). Powder SHG efficiency was measured at a fundamental wavelength of 1.9 μm relative to that of MM1 powder (about two orders of magnitude larger than urea) from Ref. [16].

	Solvent (growing method)[b]	λ_{abs} (nm)	$\lambda_{em,solution}$ (nm)	$\lambda_{em,solid}$ (nm)	T_{tr} (°C)	T_m (°C)	Powder SHG	
HP2-I	MC/MeOH, (SE)	468	575	625	170	187	2.2	This work
HP2-II	MeOH, (SE)	468	575	635	143	187	0	This work
HP2-III[a]	MeOH, (RC)	468	575	–	58, 170	184	0	This work
HP2-IV[a]	MEK, (SE)	468	575	–	60, 158, 170	184	0	This work
MP3-I	MC/MeOH, (SE)	470	575	643	134, 190	201	1.3	This work
MP3-II	AcCN, (SE)	470	575	710	134, 184	201	0	This work
MM1	MeOH (SE, RC), MG/VG	500	626	711	Not observed	236	1.0	Ref. [16]

[a] HP2-III and HP2-IV crystals include the solvent, methanol and MEK, respectively, while all other crystals listed here do not include the solvent in the crystal structure.

[b] MC (methylene chloride), MeOH (methanol), MEK (methyl ethyl ketone), AcCN (acetonitrile), RC (rapid cooling), SE (slow evaporation), MG (melt growth), VG (vapor growth).

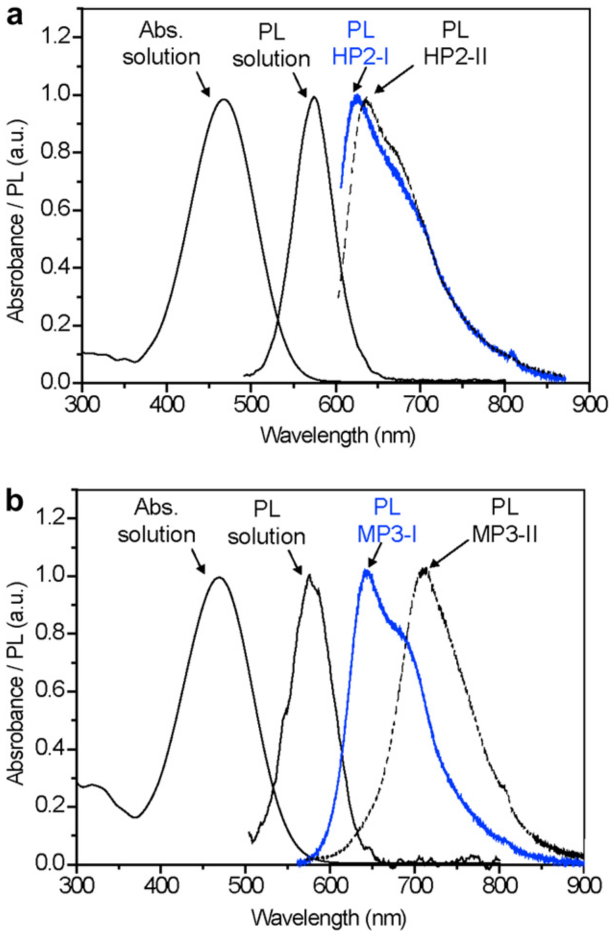

Fig. 3. Absorption and photoluminescence (PL) spectra (normalized scale) of pyrrole-based CLP derivatives in solution and in different crystalline solids: (a) HP2 and (b) MP3.

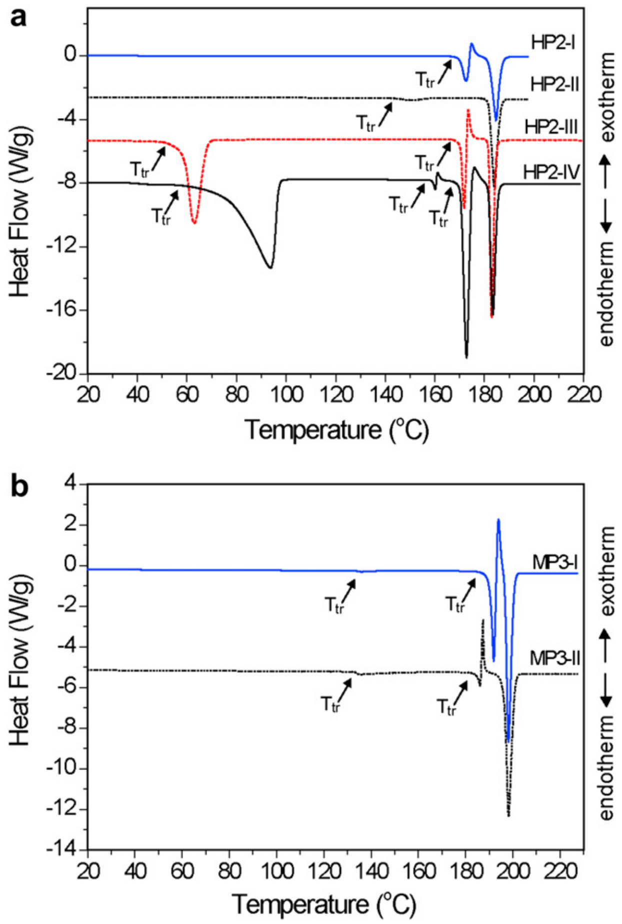

Fig. 4. DSC thermodiagrams of HP2 and MP3 crystals (10 K/min scan rate): T_{tr} is the phase transition temperature.

and MP3-I phases have a noncentrosymmetric arrangement of molecules, while the other HP2 and MP3 polymorphs have a centrosymmetric arrangement of molecules. Fig. 3 shows photoluminescence spectra of HP2 and MP3 polymorphs in solution and solid state. In solid state, the polymorphs exhibit different photoluminescence spectra: the difference of the wavelength of the maximum emission $\lambda_{em,solid}$ is 10 nm (10^6 cm^{-1}) between HP2-I and -II polymorphs and 67 nm (1.5×10^5 cm^{-1}) between MP3-I and -II polymorphs (see also Table 1). In DSC measurement we observe even more polymorphs of HP2 and MP3 crystals. Before the meting temperature, both crystals reveal several thermally induced solid–solid phase transitions (see Fig. 4).

These measurements show that the pyrrole-based chromophores having asymmetric pyrrole easily form many polymorphs. On the other hand, for MM1 crystals having a symmetric dimethylaminophenyl electron donor we only observed one crystal structure, which was obtained by various methods, e.g., by solution growth method [16,22] with slow evaporation, rapid cooling, and slow cooling in various solvents such as methanol, ethanol, acetone, methylene chloride and acetonitrile, by melt [16,23] and vapor growth [24], as well as in DSC thermodiagram measurement.

In many cases polymorphism can be induced by additives [25–28]. The reason for the occurrence of many polymorphs in pyrrole-based chromophores compared to MM1 crystal is attributed to the existence of rotational isomerization in these chromophores. Not only different rotational isomers can exist in these crystals, rotamers can lead to an additive-like effect as discussed below. The pyrrole-based chromophores having an extended π-conjugation bridge have a rotatable single bond between the pyrrole and the hexatriene bridge as illustrated in Fig. 5a [19]. The existence of rotamers was confirmed by ^{1}H NMR measurement of HP2 chromophore as shown in Fig. 5 and single-crystal X-ray analysis of HP2 and MP3 chromophores as shown in Fig. 6. In Fig. 5bc, ^{1}H NMR spectrum in $CDCl_3$ solution with different concentration of high purity materials reveals two structural features (i.e., rotamers) [19]. Fig. 6 shows the molecular structures of HP2-III and MP3-II crystals, which reveal a different conformation of the π-conjugation bridge linking pyrrole and polyene by rotational isomerization.

In solution the ratio between the NMR intensity of the minor rotamer (I_{minor}) and the major rotamer (I_{major}) decreases with increasing the solution concentration [19]. However, even in high concentration the ratio of the minor rotamer is not going to zero; for example, 6% of the minor rotamer exists in 0.1 M solution (see Fig. 5). The presence of the minor rotamer can act as a “tailor-made” additive for the major rotamer in solution. Tailor-made additives consist of the binder part with similar chemical structures and the perturber part with slightly different chemical structure disturbing hydrogen bonds of host molecules [26–28]. The fixed ratio of the rotamers at a certain solution concentration suggests that the two rotamers are in equilibrium in solution. Therefore, the minor

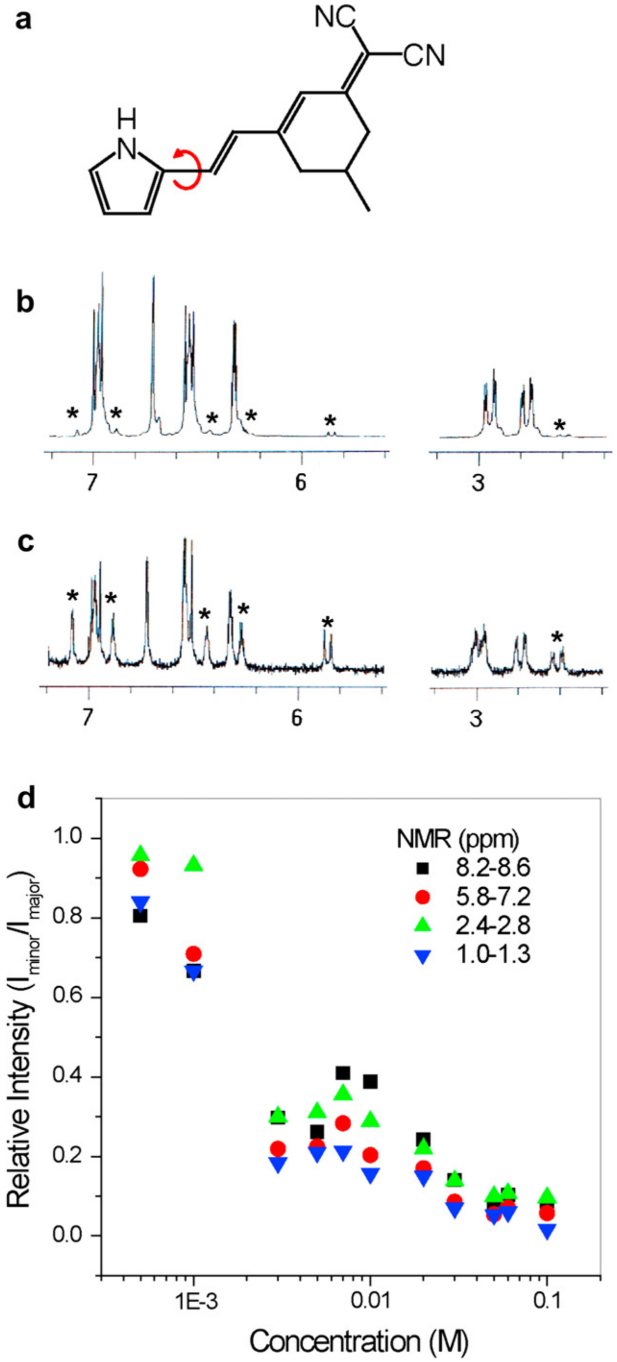

Fig. 5. The presence of rotational isomers of HP2 chromophore: (a) rotatable bond, ^{1}H NMR spectrum in $CDCl_3$ solution with different concentrations of (b) 0.06 M and (c) 0.001 M. (d) The relative NMR ratio is the ratio between the NMR intensity of the minor rotamer (I_{minor}) and the major rotamer (I_{major}). The asterisk (*) notices the minor rotamer.

rotamer, which exists even at high solution concentrations can act as an additive, i.e., the chromophore exhibits a “self-additive effect”. The minor rotamers can induce complicated hydrogen bonds with major rotamers and lead to high possibilities of complex polymorphism. Therefore, to control the molecular ordering of asymmetric pyrrolic chromophores in the solid state, the influence of rotational isomerization plays an important role in crystal characteristics and polymorphism.

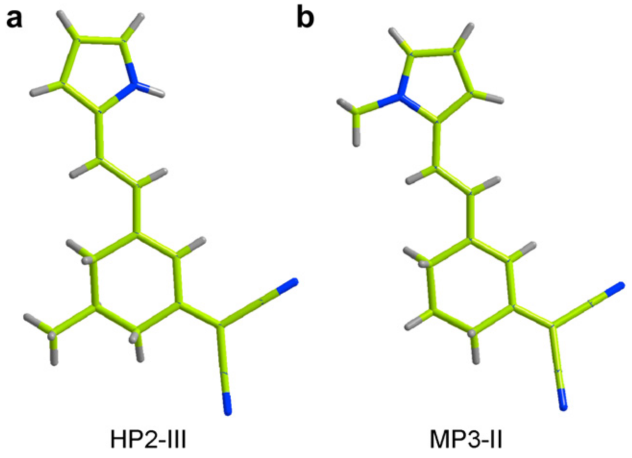

Fig. 6. Molecular structures of chromophores in HP2-III and MP3-II crystals as determined by single-crystal X-ray analysis.

4. Conclusions

To investigate acentric crystal-forming possibilities and the influence of molecular conformational change of π-conjugated bridge on crystal characteristics and polymorphism, new pyrrole-based configurationally locked polyene (CLP) derivatives with different N-substituted groups (X: $-H$, $-CH_3$) on pyrrole and with different number of methyl substituents in cyclohexene ring are designed and synthesized. The pyrrole-based HP2 crystals exhibit a large macroscopic nonlinearity with strong second harmonic generation efficiency of about two orders of magnitude larger than urea, which is promising for second-order nonlinear optical applications. We investigate the influence of pyrrole linked to the π-conjugated polyene on crystal characteristics and polymorphism. The pyrrole-based CLP chromophores having asymmetric pyrrole easily form many polymorphs, while for the CLP crystals having a symmetric dimethylaminophenyl group only one crystal structure is observed. The reason for the occurrence of complex polymorphs in pyrrole-based chromophores is attributed to the existence of rotational isomerization in these chromophores. The minor rotamer exists even at high solution concentrations and exhibits a “self-additive effect”, which induce complicated hydrogen bonds with major rotamers. Therefore, in crystal engineering of molecules having π-conjugated bridge, the influence of rotational isomerization is an important parameter.

Acknowledgement

This work has been supported by the National Research Foundation of Korea Grant (NRF) funded by the Korea government (MEST) (No. 2009-0071457), Priority Research Centers Program through the National Research Foundation of Korea (NRF) funded by the Ministry of Education, Science and Technology (2009-0093826), Ajou University Research fellowship of 2009 (20095332), and the Swiss National Science Foundation.

References

[1] Desiraju GR. Crystal engineering: a holistic view. Angewandte Chemie International Edition 2007;46(44):8342–56.
[2] Aakeroy CB, Seddon KR. The hydrogen-bond and crystal engineering. Chemical Society Reviews 1993;22(6):397–407.
[3] Aakeroy CB. Crystal engineering: strategies and architectures. Acta Crystallographica Section B-Structure Science 1997;53:569–86.
[4] Sharma CVK. Crystal engineering – where do we go from here? Crystal Growth & Design 2002;2(6):465–74.

[5] Braga D, Brammer L, Champness NR. New trends in crystal engineering. Crystal Engineering Communication 2005;7:1–19.
[6] Special Issue Polymorphism in crystals. Crystal Growth & Design 2004;4(6):1085–441.
[7] Special Issue Facets of polymorphism in crystals. Crystal Growth & Design 2008;8(1):1–362.
[8] Norikane Y, Kitamoto K, Tamaoki N. Novel crystal structure, cis–trans isomerization, and host property of meta-substituted macrocyclic azobenzenes with the shortest linkers. Journal of Organic Chemistry 2003;68(22):8291–304.
[9] Harada J, Harakawa M, Sugiyama S, Ogawa K. Single crystal cis–trans photoisomerizations of 2-(9-anthrylmethylene)-1-indanones. Crystal Engineering Communication 2009;11(7):1235–9.
[10] Li JY, Liu D, Hong ZR, Tong SW, Wang PF, Ma CW, et al. A new family of isophorone-based dopants for red organic electroluminescent devices. Chemistry of Materials 2003;15(7):1486–90.
[11] Marder SR, Beratan DN, Cheng LT. Approaches for optimizing the 1st electronic hyperpolarizability of conjugated organic-molecules. Science 1991;252(5002):103–6.
[12] Marder SR, Cheng LT, Tiemann BG, Friedli AC, Blanchare-Desce M, Perry JW, et al. Large 1st hyperpolarizabilities in push–pull polyenes by tuning of the bond-length alternation and aromaticity. Science 1994;263(5146):511–4.
[13] Ermer S, Lovejoy SM, Leung DS, Warren H, Moylan CR, Twieg RJ. Synthesis and nonlinearity of triene chromophores containing the cyclohexene ring structure. Chemistry of Materials 1997;9(6):1437.
[14] Shu YC, Gong ZH, Shu CF, Breitung EM, McMahon RJ, Lee GH, et al. Synthesis and characterization of nonlinear optical chromophores with conformationally locked polyenes possessing enhanced thermal stability. Chemistry of Materials 1999;11(6):1628–32.
[15] Staub K, Levina GA, Barlow S, Kowalczyk TC, Lackritz HS, Barzoukas M, et al. Synthesis and stability studies of conformationally locked 4-(diarylamino)aryl- and 4-(dialkylamino)phenyl-substituted second-order nonlinear optical polyene chromophores. Journal of Materials Chemistry 2003;13:825–33.
[16] Kwon OP, Ruiz B, Choubey A, Mutter L, Schneider A, Jazbinsek M, et al. Organic nonlinear optical crystals based on configurationally locked polyene for melt growth. Chemistry of Materials 2006;18(17):4049–54.
[17] Kwon OP, Kwon SJ, Jazbinsek M, Choubey A, Gramlich V, Günter P. New organic nonlinear optical polyene crystals and their unusual phase transitions. Advanced Functional Materials 2007;17(11):1750–6.
[18] Kwon OP, Kwon SJ, Jazbinsek M, Brunner FDJ, Seo JI, Hunziker Ch, et al. Organic phenolic configurationally locked polyene single crystals for electro-optic and terahertz wave applications. Advanced Functional Materials 2008;18(20):3242–50.
[19] Kwon OP, Jazbinsek M, Seo JI, Kim PJ, Choi EY, Lee YS, et al. First hyperpolarizability of asymmetric pyrrole-based polyene chromophores. Dyes and Pigments 2010;85(3):162–70.
[20] Kinnibrugh T, Bhattacharjee S, Sullivan P, Isborn C, Robinson BH, Eichinger BE. Influence of isomerization on nonlinear optical properties of molecules. Journal of Physical Chemistry 2006;110(27):13512–22.
[21] Sheldrick G. SHELXL-97. Program for the refinement of crystal structures. Germany: University of Göttingen; 1997.
[22] Kwon OP, Kwon SJ, Figi H, Jazbinsek M, Günter P. Organic electro-optic single-crystalline thin films grown directly on modified amorphous substrates. Advanced Materials 2008;20(3):543–5.
[23] Figi H, Jazbinsek M, Hunziker C, Koechlin M, Günter P. Electro-optic single-crystalline organic waveguides and nanowires grown from the melt. Optics Express 2008;16(15):11310–27.
[24] Choubey A, Kwon OP, Jazbinsek M, Günter P. High quality organic single crystalline thin films for nonlinear optical applications by vapor growth. Crystal Growth & Design 2007;7(2):402–5.
[25] Lu J, Wang XJ, Ching CB. Effect of additives on the crystallization of lysozyme and chymotrypsinogen A. Crystal Growth & Design 2003;3(1):83–7.
[26] Weissbuch I, Lahav M, Leiserowitz L. Toward stereochemical control, monitoring, and understanding of crystal nucleation. Crystal Growth & Design 2003;3(2):125–50.
[27] Torbeev VY, Shavit E, Weissbuch I, Leiserowitz L, Lahav M. Control of crystal polymorphism by tuning the structure of auxiliary molecules as nucleation inhibitors. The beta-polymorph of glycine grown in aqueous solutions. Crystal Growth & Design 2005;5(6):2190–6.
[28] Kwon OP, Jazbinsek M, Choubey A, Losio PA, Gramlich V, Günter P. Morphology and polymorphism control of organic polyene crystals by Tailor-made auxiliaries. Crystal Growth & Design 2006;6(10):2327–32.